

Supporting Information

Biocompatible photosensitizer with high intersystem crossing efficiency for precise two-photon photodynamic therapy

Zhourui Xu¹, Yihang Jiang¹, Yuanyuan Shen¹, Lele Tang², Zulu Hu¹, Guimiao Lin³, Wing-cheung Law⁴, Mingze Ma¹, Biqin Dong⁵, Ken-Tye Yong^{6,7}, Gaixia Xu¹, Ye Tao^{2,*}, Runfeng Chen^{2,*}, Chengbin Yang^{1,*}

¹Guangdong Key Laboratory for Biomedical Measurements and Ultrasound Imaging, School of Biomedical Engineering, Health Science Center, Shenzhen University, Shenzhen, 518060, China.
Email: cbyang@szu.edu.cn

²State Key Laboratory of Organic Electronics and Information Displays & Institute of Advanced Materials (IAM), Nanjing University of Posts & Telecommunications, 9 Wenyuan Road, Nanjing 210023, China
Email: iamytao@njupt.edu.cn; iamrfchen@njupt.edu.cn

³Base for International Science and Technology Cooperation: Carson Cancer Stem Cell Vaccines R&D Center, Shenzhen Key Lab of Synthetic Biology, Department of Physiology, School of Basic Medical Sciences Shenzhen University, Shenzhen, 518055, China

⁴Department of Industrial and Systems Engineering, The Hong Kong Polytechnic University, Hong Kong

⁵Guangdong Provincial Key Laboratory of Durability for Marine Civil Engineering, College of Civil and Transportation Engineering, Shenzhen University, Shenzhen, 518060, China

⁶School of Biomedical Engineering, The University of Sydney, Sydney, New South Wales 2006, Australia

⁷The University of Sydney Nano Institute, The University of Sydney, Sydney, New South Wales 2006, Australia

Table of Contents

Experimental Section

Scheme 1. The synthetic route to prepare BF₂DCz.

Scheme 2. HPLC spectra of BF₂DCz.

Figure S1. ¹H NMR spectrum of BF₂DCz in CDCl₃.

Figure S2. ¹³C NMR spectrum of BF₂DCz in CDCl₃.

Figure S3. HRMS of BF₂DCz.

Figure S4. Fluorescence emission of BF₂DCz-BSA in DI water, PBS, DMEM, FBS, and DMEM+10% FBS.

Figure S5. The hydrodynamic size of BF₂DCz-BSA in PBS and culture medium.

Figure S6. UV-vis absorption and photoluminescence spectra of BF₂DCz in different solvent.

Figure S7. UV-vis absorption and photoluminescence spectra of BF₂DCz-BSA in water.

Figure S8. The AIE characteristics of BF₂DCz.

Figure S9. Fluorescence decay profiles of BF₂DCz and BF₂DCz nanoparticles.

Figure S10. PL spectra of BF₂DCz in aerated and argon-degassed toluene solution.

Figure S11. fs-TA plots of BF₂DCz NPs.

Figure S12. The cytotoxicity evaluation of BF₂DCz-BSA.

Figure S13. The hemolysis evaluation of BF₂DCz-BSA.

Figure S14. Confocal image and two-photon image of BF₂DCz-BSA treated MCF-7 cells.

Figure S15. The cellular uptake of BF₂DCz-BSA.

Figure S16. Flow cytometry analysis of cellular uptake of BF₂DCz-BSA.

Figure S17. Fluorescence intensities of ROS indicators.

Figure S18. The PDT effect of Ce6-BSA and BF₂DCz-BSA on MCF-7 cells.

Figure S19. The morphology of MCF-7 cells treated with laser or BF₂DCz-BSA.

Figure S20. The cell survival rate of MCF-7 Cells after irradiation of 405 nm laser.

Figure S21. The intracellular singlet oxygen generation.

Figure S22. Two-photon ROS generation evaluation.

Figure S23. The two-photon images of MCF-7 cells treated with BF₂DCz-BSA.

Figure S24. The confocal images of tumor spheroids incubated with BF₂DCz-BSA.

Figure S25. Mouse model for two-photon imaging.

Figure S26. The SBR of two-photon image at specific depth.

Figure S27. Measurement of blood flow speed.

Figure S28. A selective blood vessel closure experiment in mouse brain.

Figure S29. In vivo fluorescence imaging of major organs.

Figure S30. The variation of body weight of mice.

Figure S31. Blood routine test for treated BALB/C mice.

Figure S32. Serum biochemistry assays for treated BALB/C.

Figure S33. Histological images of the major organs from mice injected with 5 mg/kg of BF₂DCz-BSA.

Figure S34. Histological images of the major organs from mice injected with 10 mg/kg of BF₂DCz-BSA.

Experimental Section:

Materials

Tetrahydrofuran (THF) solvent was purchased from Shanghai Macklin Biochemical Co., Ltd. BSA powder was purchased from Yan Cheng Sai bao Biotechnology Co., Ltd. H₂DCFHDA was purchased from R&D system, Inc. FDTMCKK-8 was purchased from Hangzhou Fude Biological Technology Co., Ltd. Calcein-AM Kit were purchased from Thermo Fisher Scientific, Inc. For the synthesis of BF₂DCz molecule, 9H-carbazole, malonyl dichloride, BF₃·Et₂O, CH₂Cl₂, and toluene were purchased from Sigma-Aldrich Co., Ltd, Acros Organics B.V.B.A., or Alfa Aesar (China) Chemical Co., Ltd. All reagents were used without further purification.

Instruments

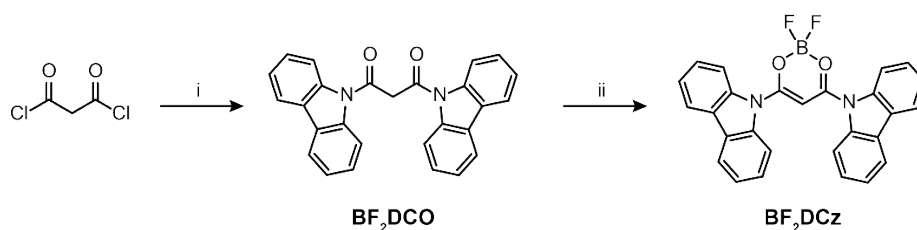
¹H and ¹³C NMR spectra were recorded on a Bruker Ultra Shield Plus 400 MHz instruments with CDCl₃ as the solvents and tetramethylsilane (TMS) as the internal standard. High-resolution mass spectra were collected by a LCT premier XE (Waters) HRMS spectrometry. UV-vis and photoluminescence spectra were recorded using TP-720 (Tian Jin Tuo Pu Instruments Co., Ltd) and F-4600 (HITACHI, Ltd) respectively. The morphology and composition of nanoparticles were analyzed by a field emission transmission electron microscope (F200, JEOL Ltd.). Hydrodynamic diameter and polydisperse index were measured by dynamic light scattering (DLS) with Zetasizer-Nano-ZS90 (Malvern Instruments Ltd.) at room temperature. Fluorescent images of cell samples were captured by fluorescent microscope (Axio Vert. A1, Carl Zeiss Co., Ltd.) and Ultra-high resolution confocal microscope (ZEISS-LSM880). Multiphoton microscope (A1MP, Nikon Co., Ltd.) with tunable femtosecond laser source (700-1080 nm, 120 fs, 80 MHz, 1 W) was used for *in vitro* and *in vivo* experiments for two-photon excited imaging and photodynamic therapy.

The synthesis of 1, 3-di(9H-carbazol-9-yl) propane-1, 3-dione (BF₂DCO)

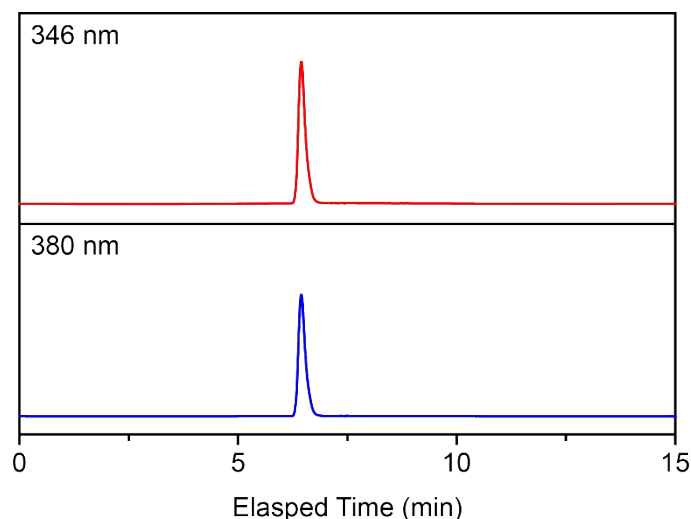
To a 50 mL round-bottom flask charged with 9H-carbazole (1.00 g, 6.0 mmol) was injected 30 mL dry toluene using a syringe under an argon atmosphere. Then, the malonyl dichloride (0.29 mL, 3.0 mmol) was injected to the toluene solution slowly. After stirring at room temperature for 5 min, the reaction was finished and the resulting DCzDCO in white precipitates was collected by filtration under reduced pressure. The precipitates were washed with sufficient acetone to remove the unreacted carbazole to obtain the purified DCzDCO for the next reaction. Yield: 0.90 g of white powder (75%).

The synthesis of difluoroboron 1, 3-di(9H-carbazol-9-yl)propane-1, 3-dione (BF₂DCz).

To a solution of DCzDCO (0.50 g, 1.2 mmol) in 40 mL dichloromethane (CH₂Cl₂) was added BF₃·Et₂O (0.46 mL, 3.6 mmol) under a dry argon atmosphere. The mixture was refluxed overnight. Then, the reaction was quenched by cooling to room temperature and washing with water (30 mL). The reaction mixture was extracted with CH₂Cl₂ (3×30 mL) and the organic layers were collected and dried with anhydrous Na₂SO₄. After removing the solvent by vacuum-rotary evaporation, the solid residue was purified by column chromatography (silica gel, 3:1 v/v, petroleum ether/ CH₂Cl₂). Yield: 0.35 g of green powder (65%). ¹H NMR (400 MHz, CDCl₃): δ 8.24 (d, J = 8.0 Hz, 4H), 8.05 (d, J = 8.0 Hz, 4H), 7.57 (t, J = 16 Hz, 4H), 7.48 (t, J = 16 Hz, 4H), 6.79 (s, 1H). ¹³C NMR (100 MHz, CDCl₃): δ 167.7, 137.86, 127.88, 127.2, 125.13, 120.57, 115.89, 80.27. HRMS (ESI): *m/z* calcd. for C₂₇H₁₈BF₂N₂O₂ [M+H]⁺, 451.1429; found, 451.1437.



Scheme 1. The synthetic route to prepare **BF₂DCz**. The reaction conditions: (i) toluene, room temperature; (ii) BF₃·Et₂O, CH₂Cl₂, room temperature.



Scheme 2. HPLC spectra of BF₂DCz monitored at the onset absorption of 346 nm and 380 nm with acetonitrile (ACN)-water as eluent in a ratio of 50/50 (v/v).

The fabrication of BF₂DCz-BSA nanoparticles.

BF₂DCz molecules (0.5 mg) were firstly dissolved in THF (0.5 mL) and then added into BSA solution (1 mg/mL, 5 mL) under vigorous stirring. The obtained BF₂DCz-BSA nanoparticles were purified and collected by ultrafiltration with molecular cut-off of 100K Da under 4.4k rpm for 20 minutes. The BF₂DCz-BSA nanoparticles were further filtrated through 0.45 μm syringe filter and suspended in PBS solution with the concentration of 1 mg/mL. The BF₂DCz-BSA nanoparticles were stored in 4°C prior to use.

Cell culture, BF₂DCz-BSA nanoparticles treatment, intracellular ROS evaluation, in vitro PDT efficiency estimation.

MCF-7 cells were grown into the glass-bottom dishes using advanced DMEM (brand), supplemented with 10% fetal calf serum (FBS) (brand), 1% Penicillin-Streptomycin Solution (PS) (brand) at 37 °C in a humidified atmosphere containing 5% CO₂. In all cellular experiments, the laser power delivered to the sample was estimated to be 4 mW, and the dose of laser radiation is depending on the exposure area (for a typical exposure area of 200 μm×200 μm, the dose of laser radiation is about 45 J/cm² per scan). Prior to the measurement of intracellular ROS generation, MCF-7 cells were incubated with BF₂DCz-BSA nanoparticles (the concentration of nanoparticles is 10 ppm based on the amount of BF₂DCz molecules) for 4 hours. The treated MCF-7 cells were washed three times with PBS buffer to remove the residual nanoparticles and supplemented with fresh culture medium, and then incubated with H₂DCFDA (5 μM) for 30 minutes. After washing

three times with PBS buffer and supplemented with fresh medium, the cells were processed for two-photon excitation and the measurement of intracellular ROS generation. Prior to *in vitro* TP-PDT treatment, MCF-7 cells were incubated with BF₂DCz -BSA nanoparticles (the concentration of nanoparticles is 10 ppm based on the amount of BF₂DCz molecules) for 4 hours. The treated MCF-7 cells were washed three times with PBS buffer to remove the residual nanoparticles and supplemented with fresh culture medium. The cell samples were then exposed to 800 nm femtosecond laser for different time period. The exposed cell samples were further cultured for 2 hours and then incubated with Calcein-AM (2 μM) and PI (2 μM) for 15 minutes. Finally, the cells were washed three times with PBS buffer before imaging.

The preparation of tumor spheroid

Soft-Agar Spheroid Assay: Soft-Agar spheroid formation assay was performed according to our previous experience with minor modifications. Briefly, 1000 single MCF-7 cells were mixed with 0.3% low melting point agarose gel containing 10% FBS. Then, the cells were seeded in 35 mm Petri dishes that were precoated with 0.6% low melting point agarose gel containing 10% FBS. The cells were then further cultured for four weeks to form 3-dimensions tumor spherical colony. Afterward, the cell spheroids were treated with different materials, and the intensity and distribution of fluorescence in formatted spheroids were analyzed under an inverted fluorescent confocal microscope.

Fluorescence Microscopic Imaging of Mice Brain Vasculature.

Female white mice (BALB/c) were obtained from the Laboratory Animal Center of Shenzhen University (Shenzhen, China). Mouse with cranial window was prepared with the following steps. All surgical instruments and supplies used in the cranial window surgery were sterilized. Before the surgery, the skin was sterilized by wiping the operating area with three alternating swipes of 70% alcohol and betadine. The ointment was applied to the eyes to prevent them from drying. Mice were injected subcutaneously with dexamethasone. Afterwards, the craniotomy was performed using a microdrill to open the skull with a circle of about 4 mm. Then the piece of skull was removed and cold saline-soaked gelfoam was applied to the dura matter to stop the small bleeding. Then a glass cover slip was gently laid on the top of dura matter and a drop of cyanoacrylate glue was applied around the coverslip to seal the window. After drying, the skull surface was covered with dental acrylic. Antibiotics were administered every day after surgery for 4-5 days. Each mouse was further housed in single cage and fed with standard mouse chow and water for more than a week before conducting two-photon experiments.

For *in vivo* brain blood vessel imaging and closure experiment, the mice were fixed in a brain stereotaxic frame after anesthetized with 1% sodium pentobarbital and a heating pad was used to maintain the body temperature. After 3-5 minutes, the mouse was injected with 5 mg/kg BF₂DCz -BSA nanoparticles via intravenous injection. After 10 minutes of injection, the treated mouse was immobilized using a lab-built scaffold and put under the microscope for two-photon imaging and brain blood vessel closure (Figure S). A multiphoton microscope (NIKON-AIMP) equipped with the 800 nm fs laser (120 fs, 80 MHz, 1 W) was used. A water-immersion objective (40 ×, NA = 1.05) was used to focus the laser beam to image the brain blood vessel. The laser irradiation delivered to the focal plane was about 40 mW. For two-photon imaging of brain blood vessel, a section of the artery was irradiated as a series of 318 × 318 μm images, each 2 μm apart through the

depth, and total scan depth was 379 μm . For blood vessel closure, an artery with a diameter of 5 μm in the depth of 100 μm were selected. The middle part of artery was selected and exposed with 800 nm laser for continuously 4 minutes. The two-photon images of the irradiated-artery before and after irradiation were compared.

The protocol of animal experiments was approved by the Institutional Ethical Committee of Animal Experimentation of Shenzhen University in China, and the experiments were performed strictly according to governmental and international guidelines on animal experimentation. According to requirements for Biosafety and Animal Ethics, all efforts were made to minimize the number of animals used and their suffering.

***In vivo* toxicology evaluation**

In vivo toxicity was carried out by using BALB/C mice ($n=5$), each of which was injected either BF2BCz-BSA (three different dosages: 5, 10, and 20 mg/kg) or PBS (control). The body weight of mice was recorded for 15 days. On day 15, all mice were sacrificed, and the blood was taken. Hematological indicators were characterized on chemistry analyzer. H&E staining of major organ slices were performed after fixing them in 10% formalin for 2 days.

Statistical analysis

Data were indicated as means \pm SD. Statistical analysis was performed using ANOVA. The statistical significance was examined by Student's t-test when two groups were compared. Statistical analysis was considered significant differences when P values less than 0.05.

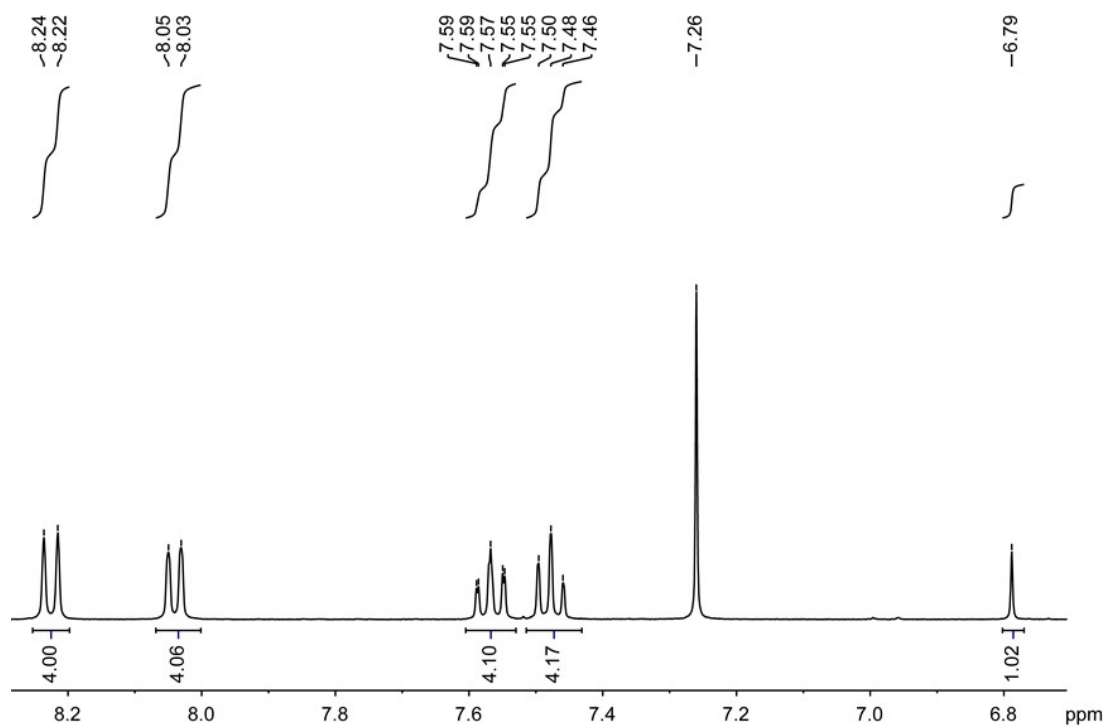


Figure S1. ^1H NMR spectrum of BF_2DCz in CDCl_3 .

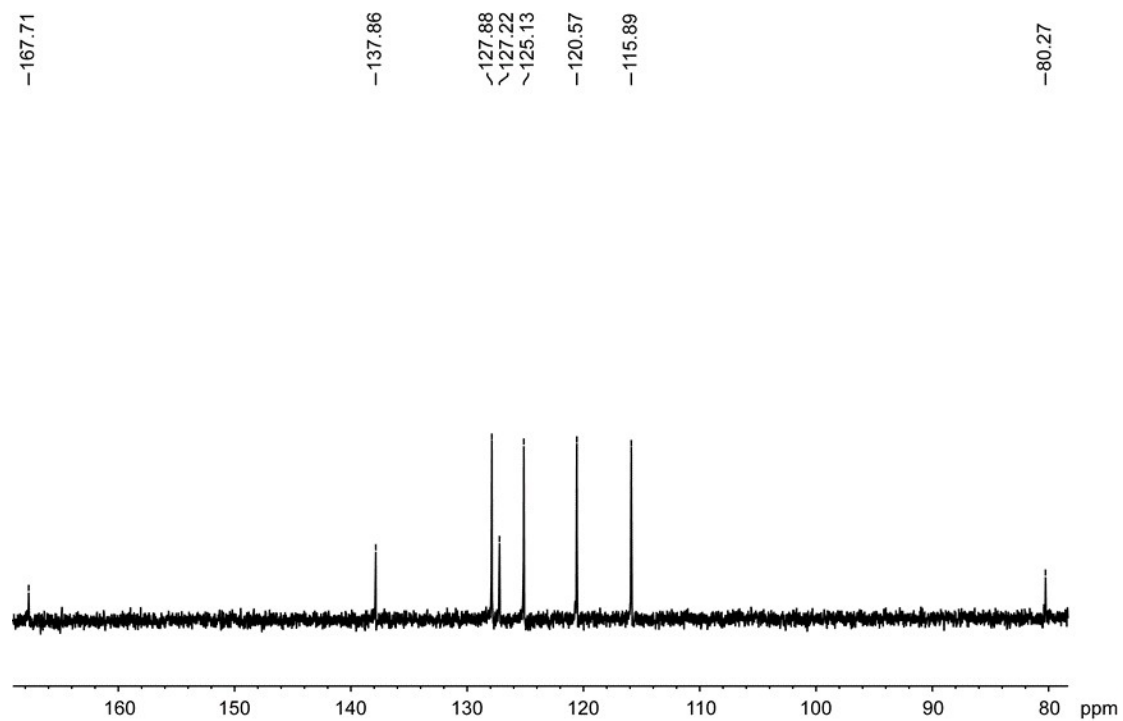


Figure S2. ^{13}C NMR spectrum of BF_2DCz in CDCl_3 .

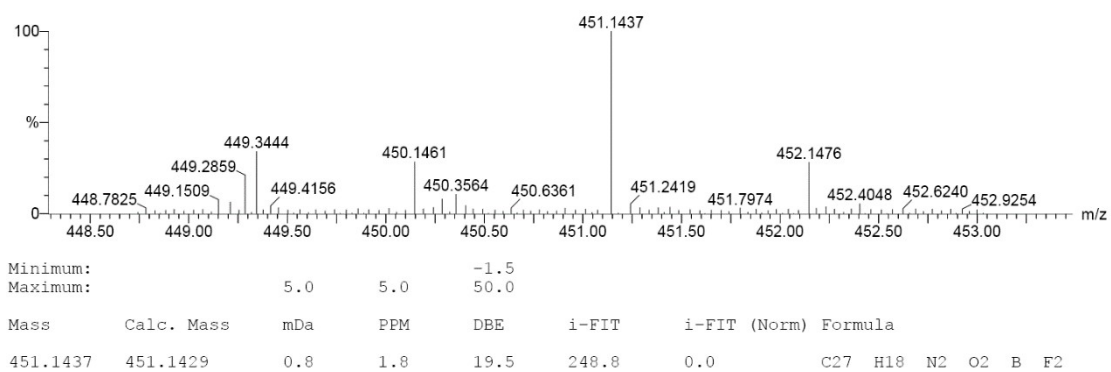


Figure S3. HRMS of BF₂DCz.

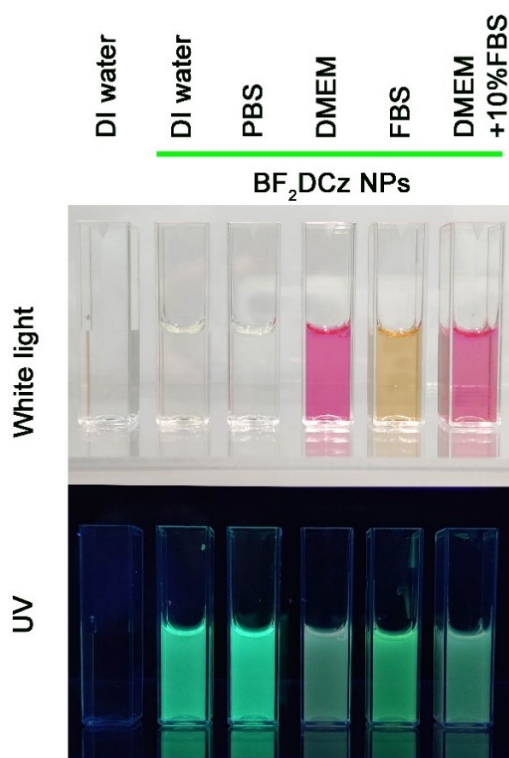


Figure S4. BF₂DCz-BSA are dispersed in diverse types of physiological solutions (DI water, PBS, DMEM, FBS, and DMEM+10% FBS) and its fluorescence under 365 nm UV light irradiation.

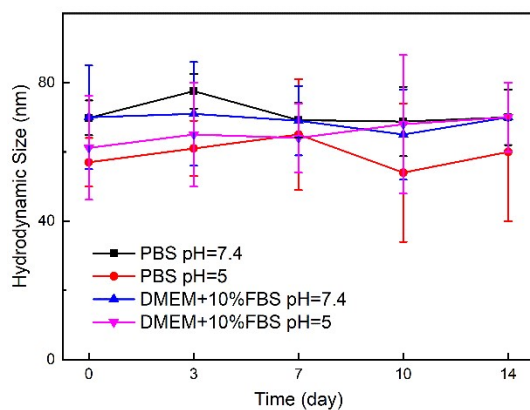


Figure S5. The hydrodynamic size of BF₂DCz-BSA in PBS and culture medium (DMEM+10%FBS) at neutral and acidic conditions within 14 days.

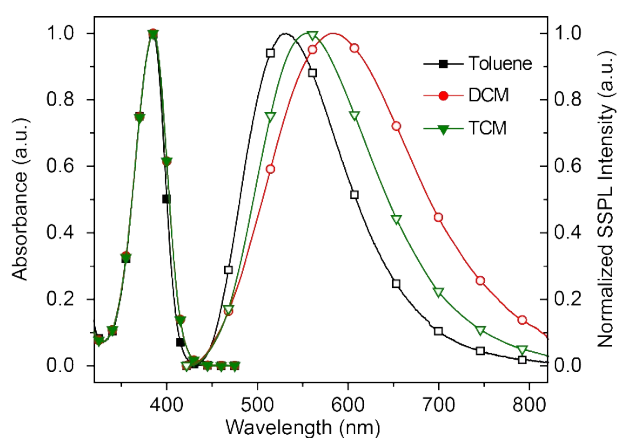


Figure S6. UV-vis absorption (solid symbols) and steady-state photoluminescence spectra (SSPL, open symbols) of BF₂DCz different solvent of toluene, CH₂Cl₂ (DCM) and chloroform (TCM) at room temperature.

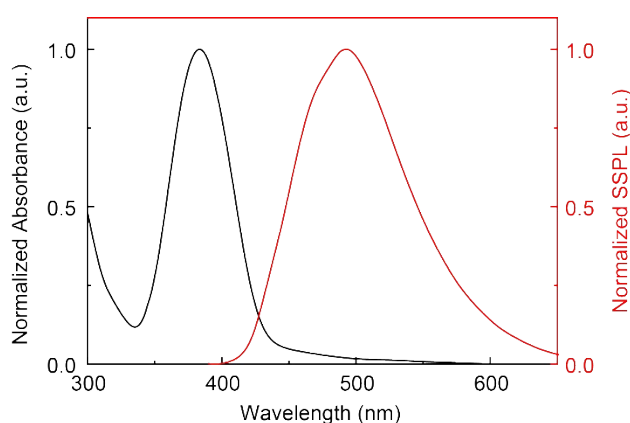


Figure S7. UV-vis absorption (black) and SSPL spectra (red) of BF₂DCz-BSA in water at room temperature.

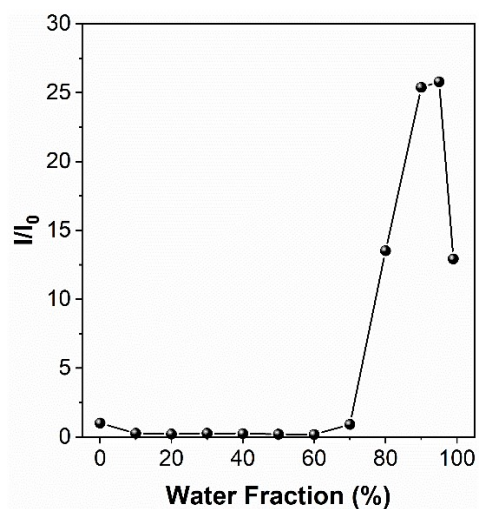


Figure S8. The AIE characteristics of BF₂DCz in THF/water solvent system.

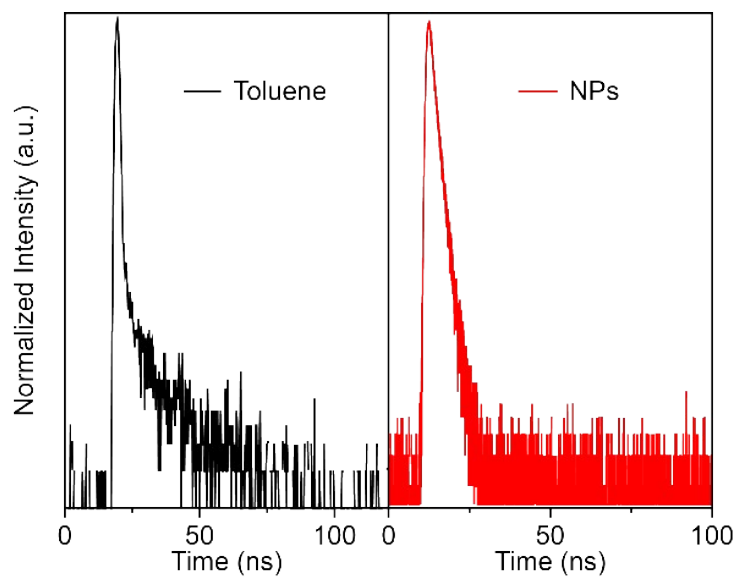


Figure S9. Fluorescence decay profiles of BF₂DCz molecules in (black) toluene and BF₂DCz nanoparticles (right) in water excited by 290 nm laser at room temperature.

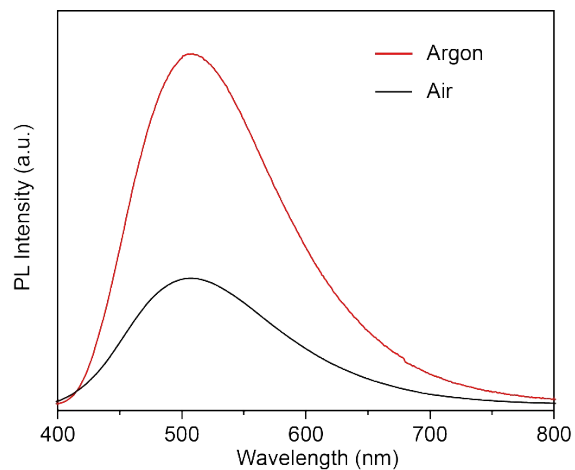


Figure S10. PL spectra of BF₂DCz in aerated and argon-degassed toluene solution.

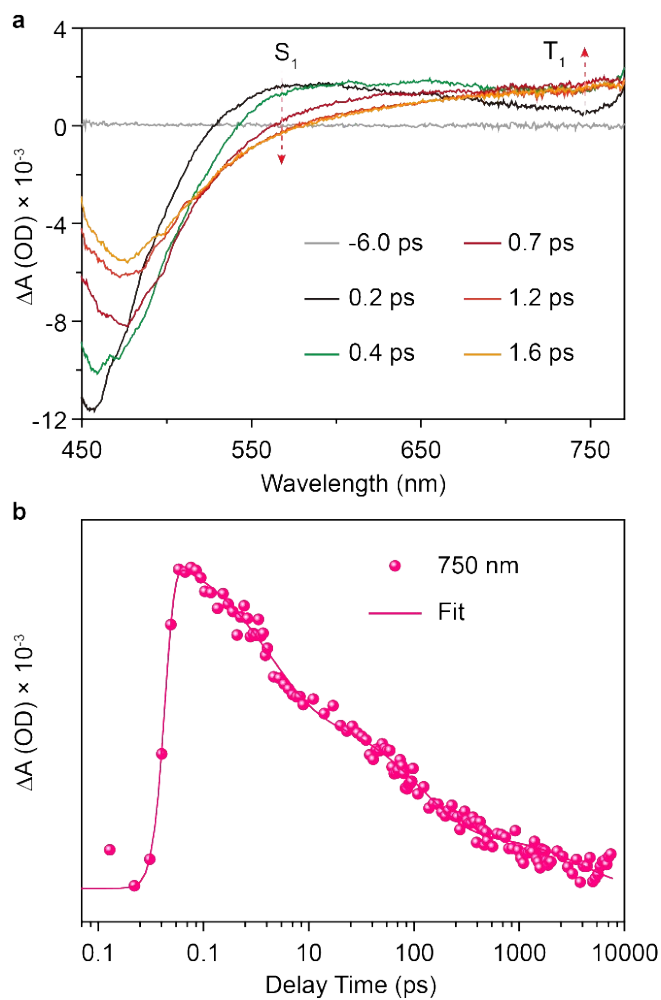


Figure S11. (a) fs-TA plots of BF₂DCz NPs at different pump-probe delay times. (b) Population dynamics of the triplet excited state at 750 nm.

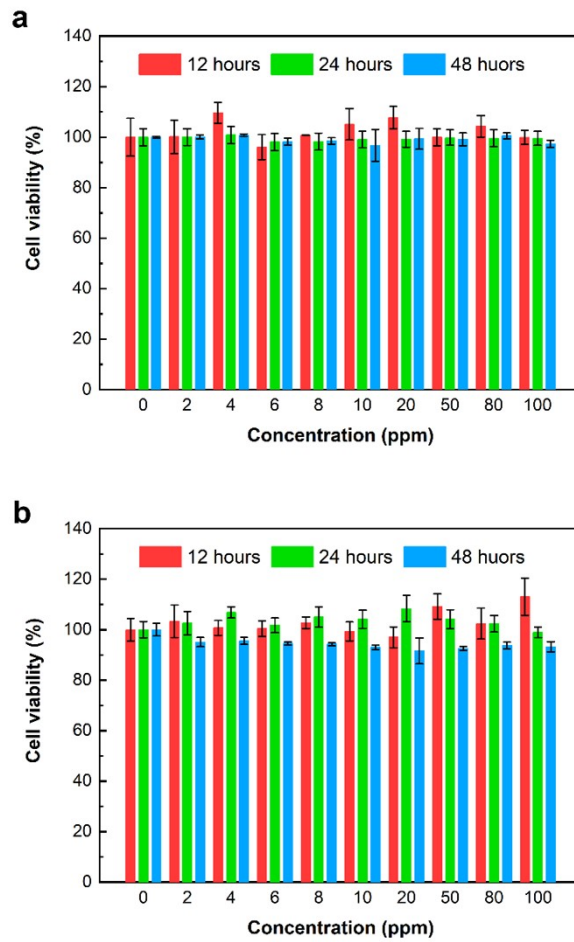


Figure S12. The cytotoxicity of BF₂DCz-BSA is evaluated on (a) HeLa and (b) MCF-7 cells. Nanoparticles with diverse concentrations were used to assess their cytotoxicity in 12, 24, and 48 hours.

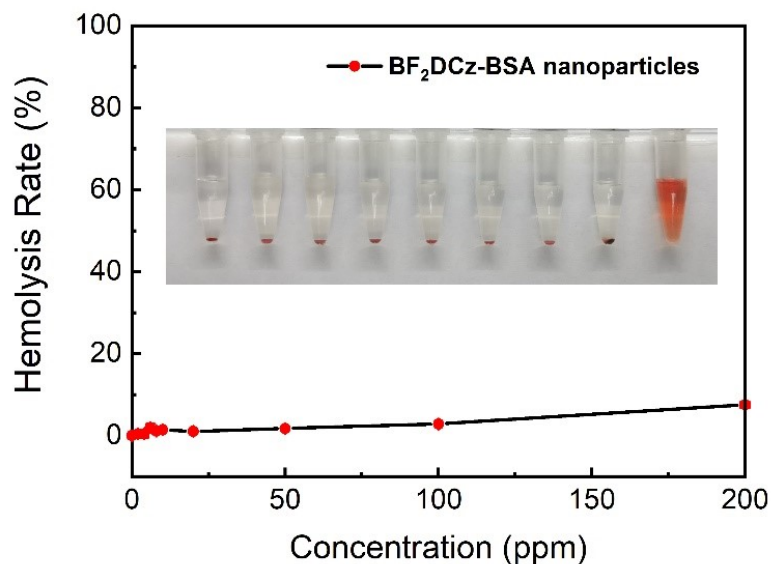


Figure S13. The hemolysis rate of blood cells induced by BF₂DCz-BSA with diverse concentrations. PBS buffer was used as negative control and DI water was used as positive control.

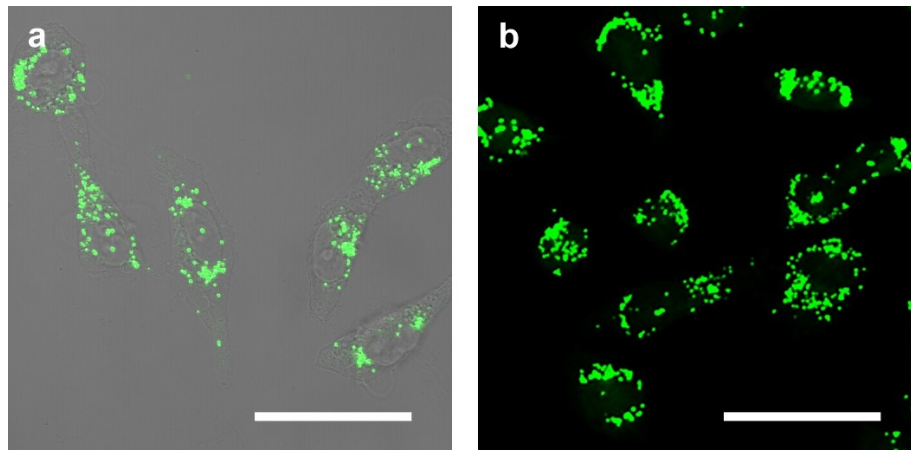


Figure S14. (a) The confocal image and (b) two-photon image of MCF-7 cells after incubated with BF₂DCz-BSA for 4 hours. (Scale bar is 25 μm)

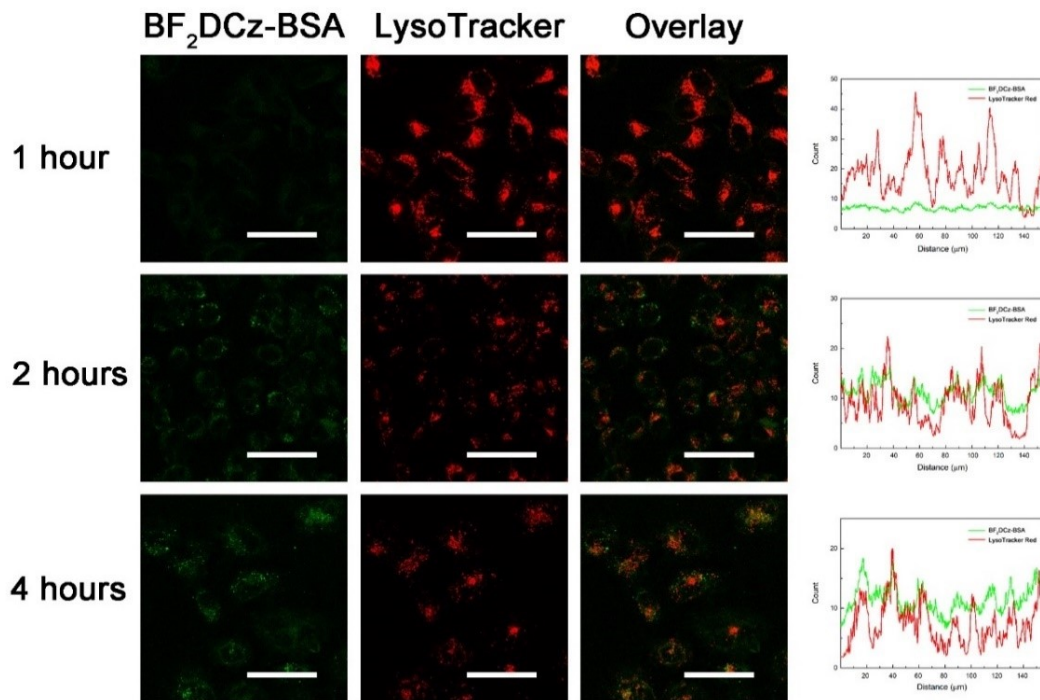


Figure S15. The cellular uptake of BF₂DCz-BSA at different time point at 4°C. The LysoTracker dye indicates the amounts and locations of lysosome. (Scale bar is 25 μm)

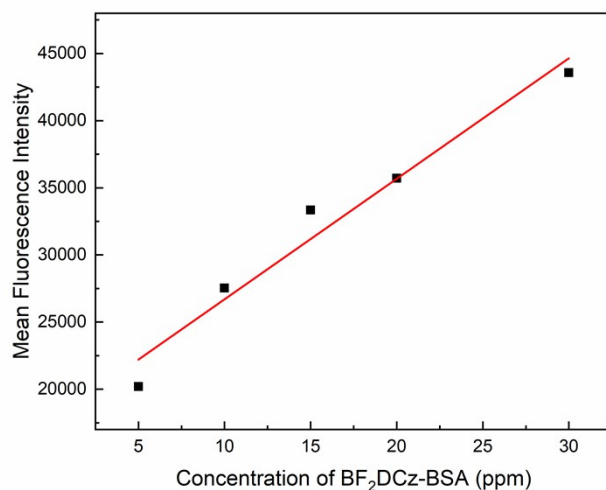


Figure S16. The relationship between the concentration of BF₂DCz-BSA applied to cells and the mean fluorescence intensity in MCF-7 cells.

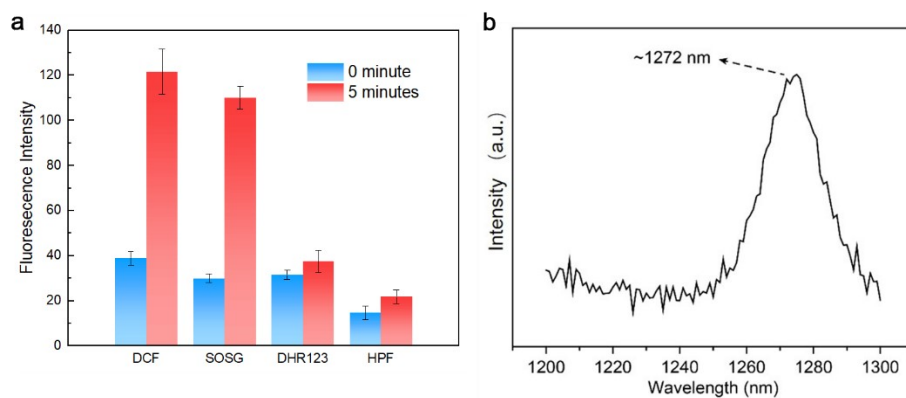


Figure S17. a) fluorescence intensities of ROS indicators (DCF, SOSG, DHR123, HPF) before and after irradiation of 5 minutes. b) phosphorescence spectral signal of singlet oxygen.

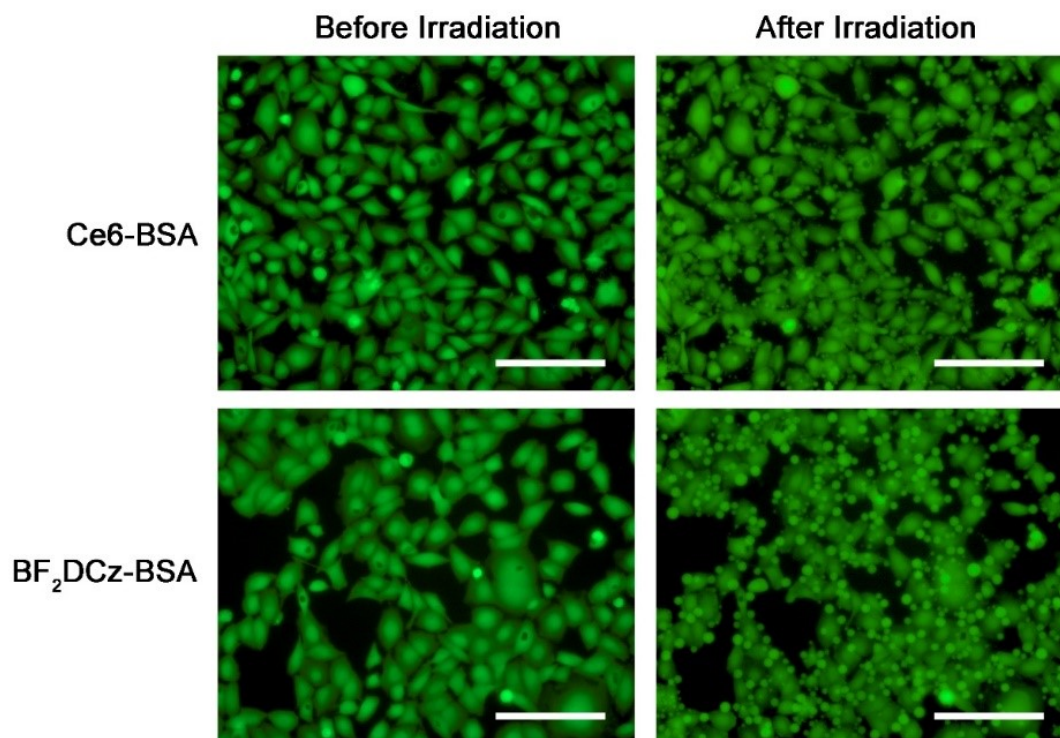


Figure S18. The PDT effect of Ce6-BSA and BF₂DCz-BSA on MCF-7 cells triggered by single photon excitation (405 nm laser of fluorescent microscope). The green fluorescence is originated from Calein-AM. (Scale bar is 50 μ m)

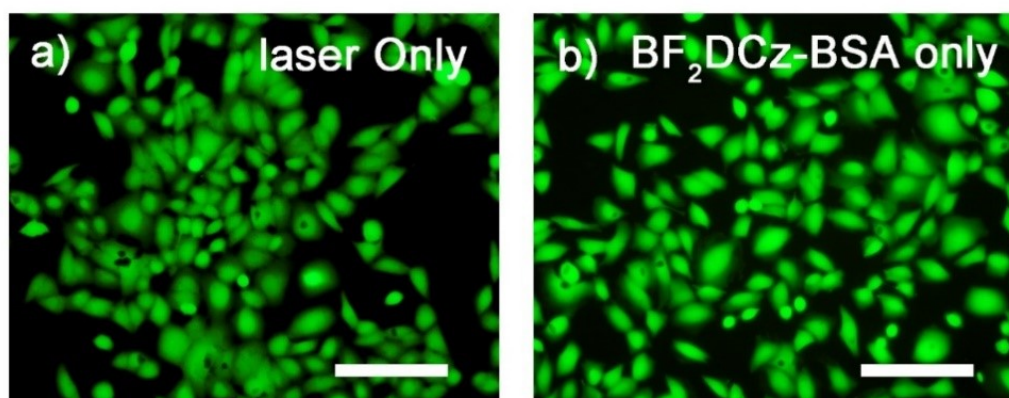


Figure S19. The morphology of MCF-7 cells treated with (a) laser only (405 nm laser of confocal microscope) or (b) BF₂DCz-BSA only appeared normal without membrane deformation. The green fluorescence is originated from Calein-AM. (Scale bar is 50 μ m)

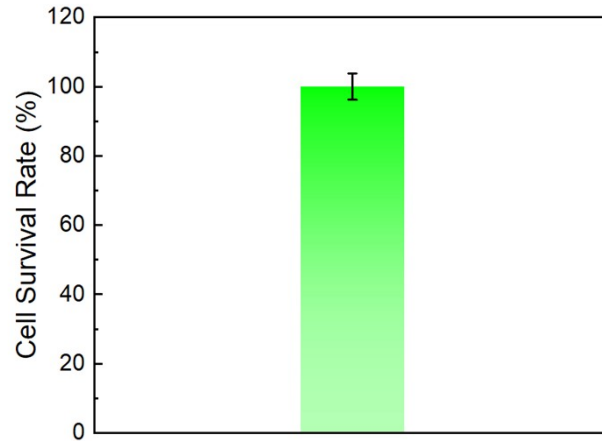


Figure S20. The cell survival rate of MCF-7 Cells after irradiation of 405 nm laser for continuously 10 minutes.

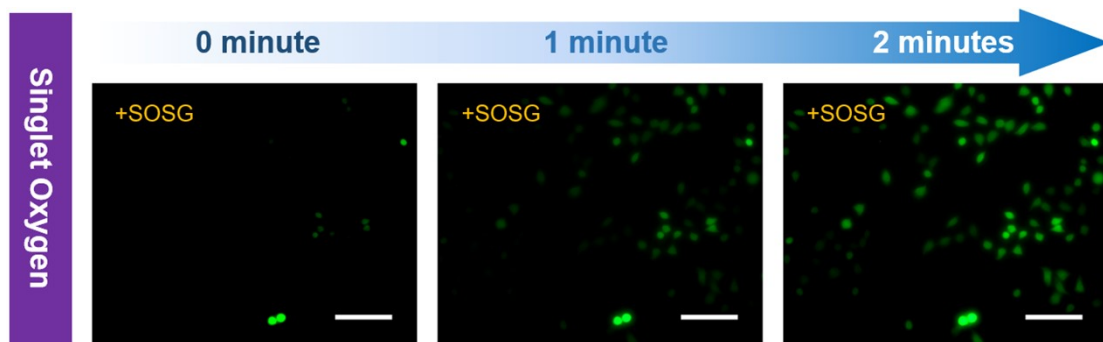


Figure S21. The intracellular singlet oxygen generation by using SOSG dye under the irradiation of 405 nm laser. (Scale bar: 100 μm)

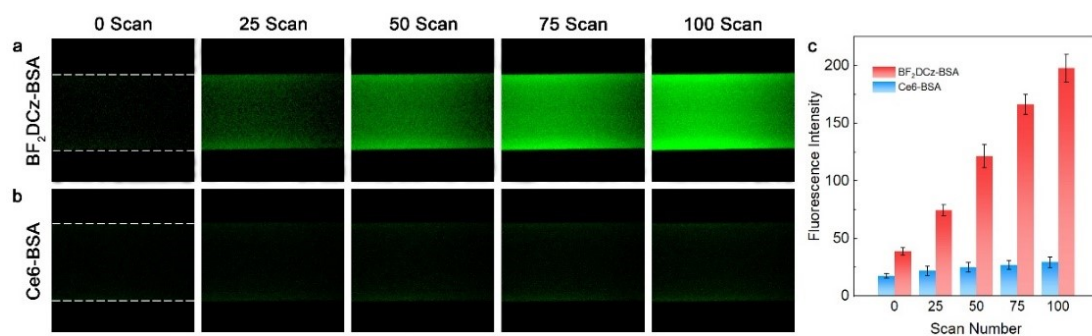


Figure S22. Two-photon fluorescence images of DCF in the aqueous medium of (a) BF₂DCz-BSA and (b) Ce6-BSA after different laser scan numbers (30 J cm⁻² per scan). (c) The two-photon fluorescence intensities of DCF calculated based on the images in panels a and b. Excitation lasers for two-photon fluorescence images: 800 nm for BF₂DCz-BSA and Ce6-BSA, and 900 nm for DCF.

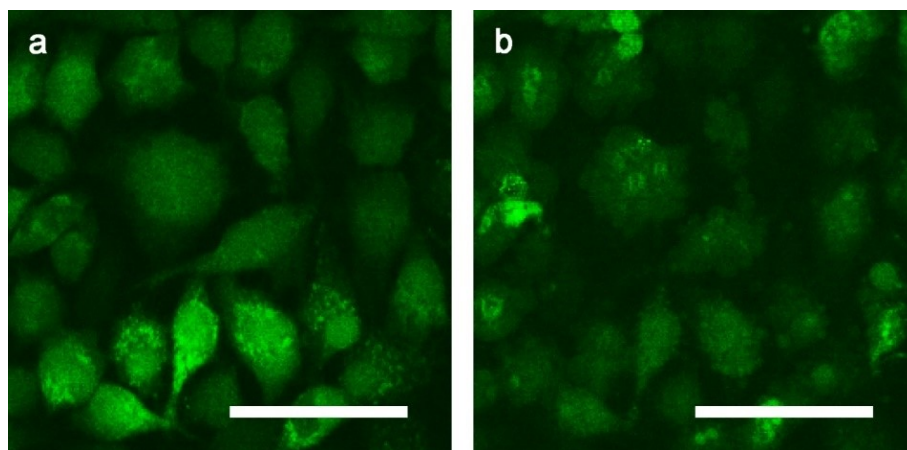


Figure S23. The two-photon images of MCF-7 cells treated with BF₂DCz-BSA (a) before and (b) after 40 second of 800 nm laser irradiation. Small blebs appeared on the laser exposed cell. (Scale bar is 50 μm)

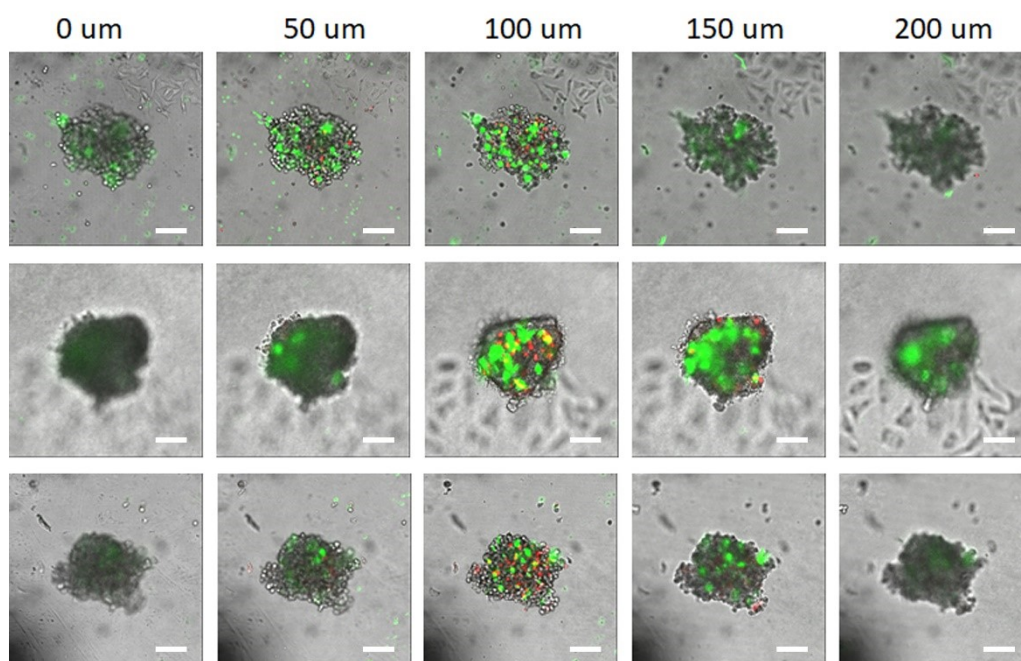


Figure S24. The confocal images of three independent tumor spheroids which have been incubated with BF₂DCz-BSA and exposed under 800 nm femtosecond laser at penetration depth of 100 μm. The green fluorescence indicates the location of BF₂DCz-BSA and red fluorescence indicates necrotic cells. (Scale bar, 50 μm)

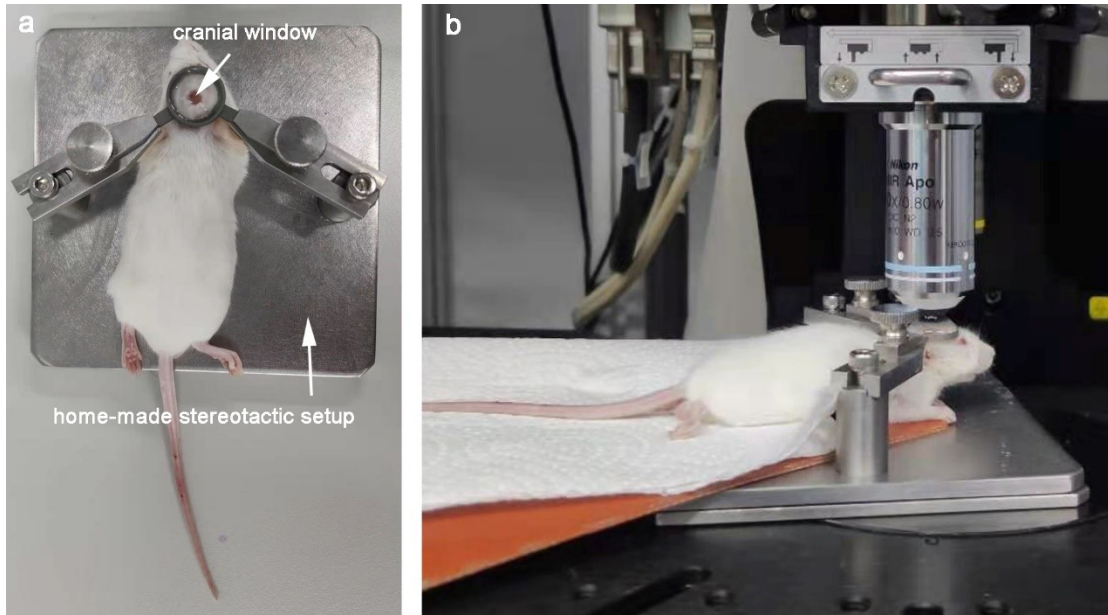


Figure S25. (a) Mouse with cranial window was immobilized on a home-made stereotactic setup and (b) imaged using a 40× water lens.

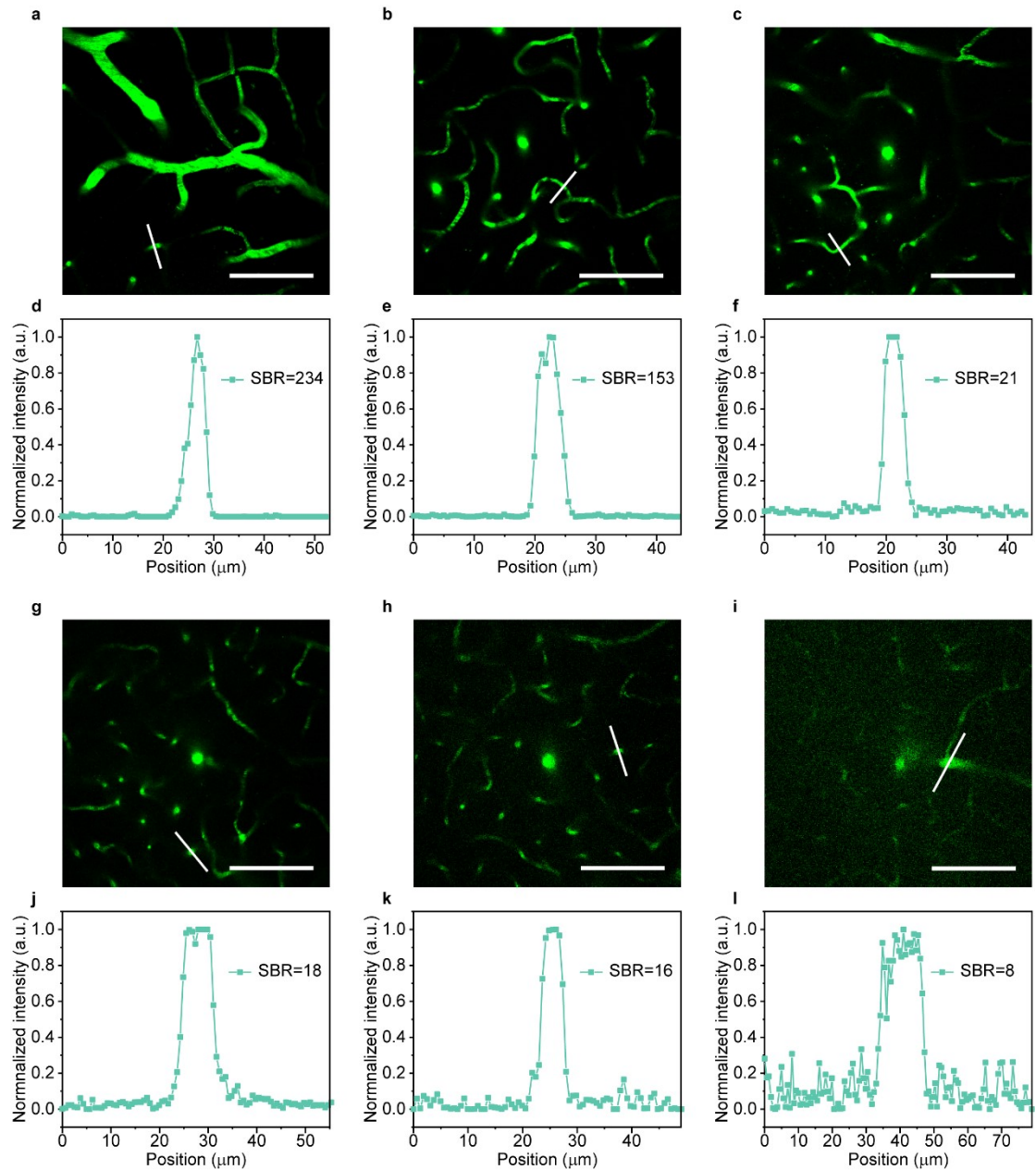


Figure S26. The brain vascular imaging at depth of (a) 30 μm , (b) 100 μm , (c) 200 μm , (g) 300 μm , (h) 400 μm , (i) 500 μm . (d-f, j-l) The corresponding SBR of each image was calculated by comparing the average fluorescence intensity from $\text{BF}_2\text{DCz-BSA}$ and the background signals. (Scale bar is 100 μm)

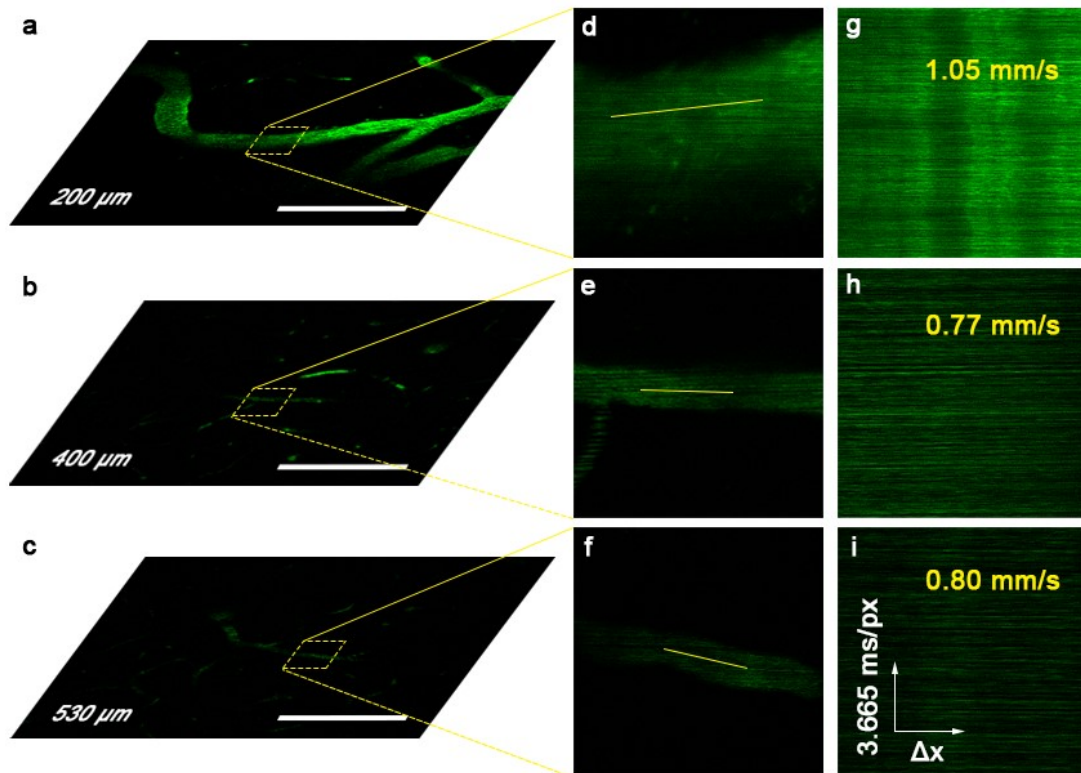


Figure S27. Measurement of blood flow speed. Blood vessels at depth of (a) 200 μm , (b) 400 μm , and (c) 530 μm were selected as representatives. (d-f) Line scan was applied along the blood vessels and (g-i) the flow speed was calculated by measuring the slope of tilted stripes. (Horizontal direction: 0.07 $\mu\text{m}/\text{px}$; vertical direction: 3.665 ms/px)

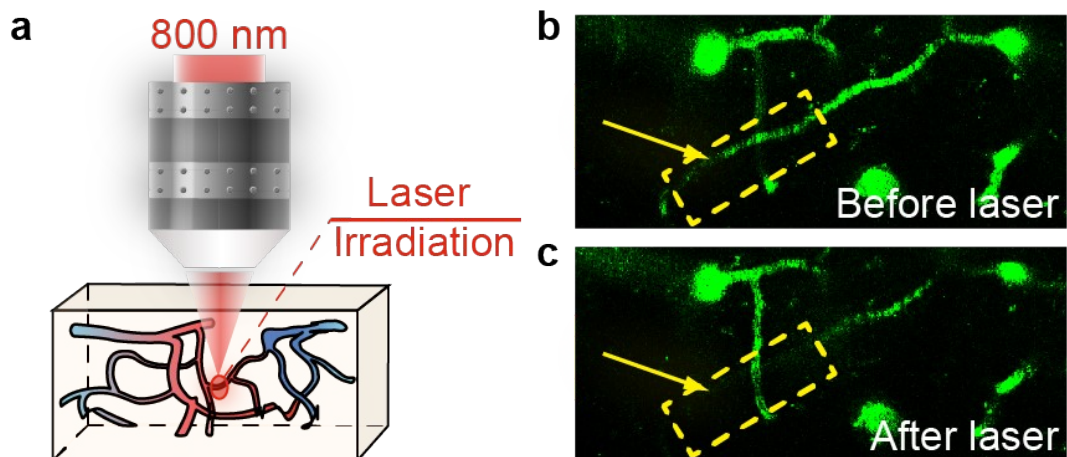


Figure S28. A selective blood vessel closure experiment in mouse brain triggered by TP-PDT. (a) Before and (b) after laser irradiation of a blood vessel at the depth of 100 μm .

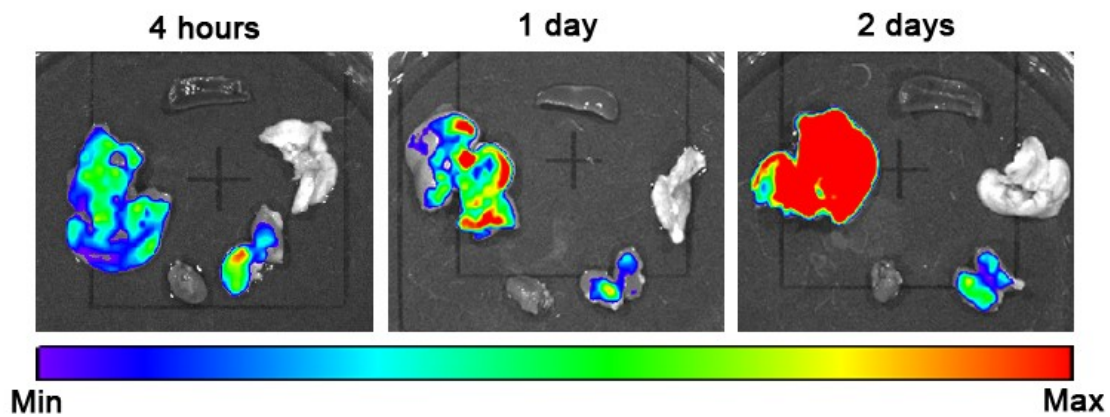


Figure. S29. In vivo fluorescence imaging of major organs (liver, spleen, lung, kidney, and heart) of mice which treated with BF₂DCz-BSA after different time duration.

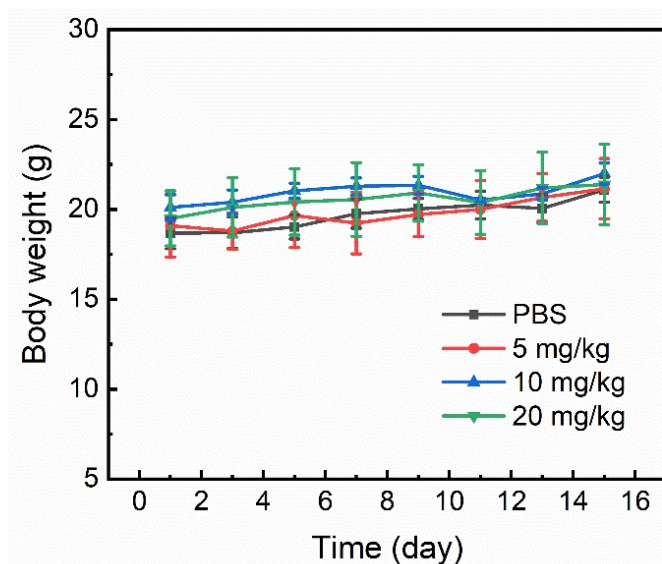


Figure S30. The variation of body weight of mice in 15 days, after injection of PBS buffer or BF₂DCz-BSA of three dosage schemes.

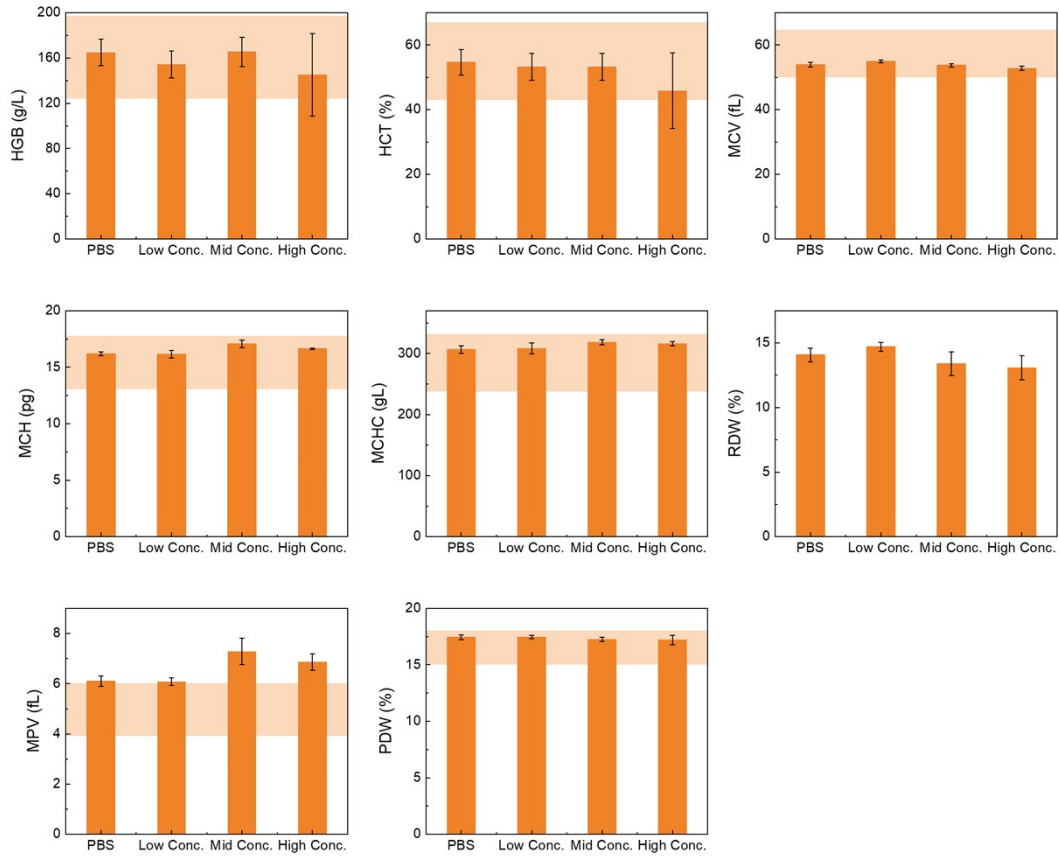


Figure S31. Blood routine test for treated BALB/C mice (n=5). The region rendered in pale orange represents the normal range from the literature. Abbreviations: hemoglobin, HGB; red blood cell specific volume, HCT; mean corpuscular volume, MCV; mean corpuscular hemoglobin, MCH; mean corpuscular hemoglobin concentration, MCHC; red cell distribution width, RDW; mean platelet volume, MPV; platelet distribution width, PDW.

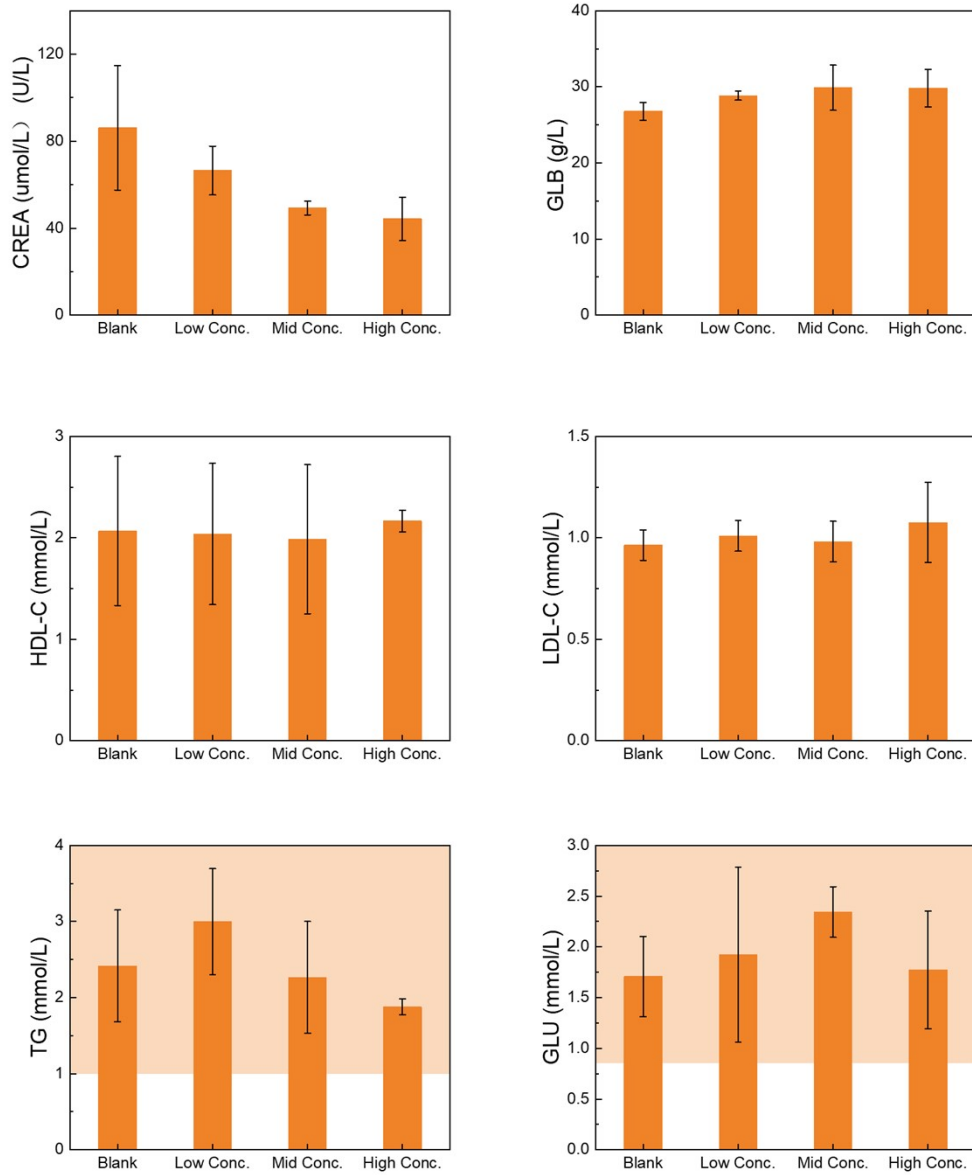


Figure S32. Serum biochemistry assays for treated BALB/C mice (n=5). The region rendered in pale orange represents the normal range from the literature. Abbreviations: creatinine, CREA; serum globulin, GLB; high-density lipoprotein, HDL-C; low-density lipoprotein LDL-C; triglyceride, TG; glucose, GLU.

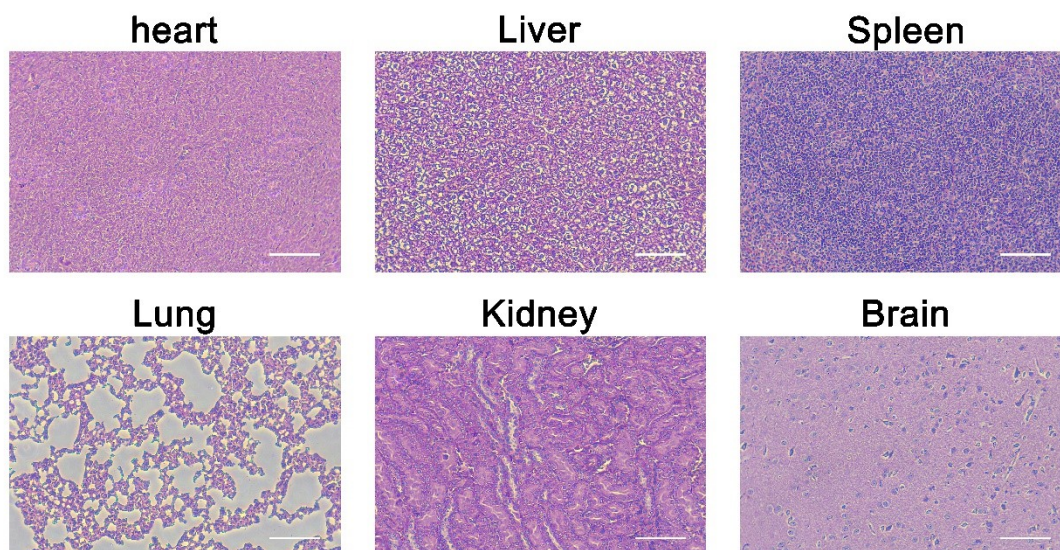


Figure S33. Histological images of the major organs (heart, liver, spleen, lung, kidney, and brain) of mice at the end of 15 days after intravenous injection of BF₂DCz-BSA suspension with dosage of 5 mg/kg. (Scale bar is 100 μ m)

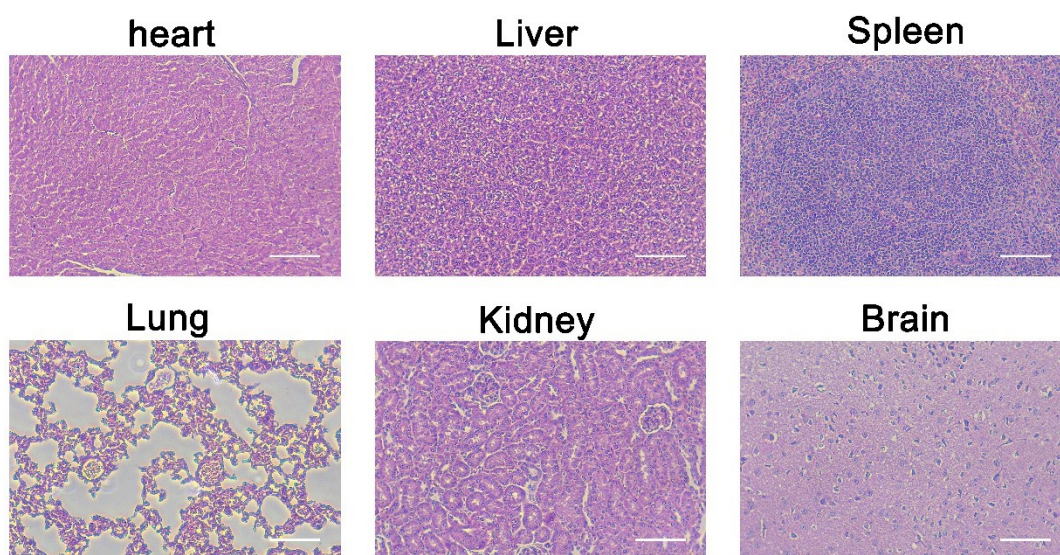


Figure S34. Histological images of the major organs (heart, liver, spleen, lung, kidney, and brain) of mice at the end of 15 days after intravenous injection of BF₂DCz-BSA suspension with dosage of 10 mg/kg. (Scale bar is 100 μ m)